

## **Evaluation of tungsten transport and concentration control in ITER scenarios**

A. Loarte<sup>1</sup>, M. Hosokawa<sup>1</sup>, A. Polevoi<sup>1</sup>, P. de Vries<sup>1</sup>, F. Köchl<sup>2</sup>, V. Parail<sup>3</sup>, E. Belli<sup>4</sup>,  
J. Candy<sup>4</sup>, G. Staebler<sup>4</sup>, R. Dumont<sup>5</sup>, D. Zarzoso<sup>6</sup>, E. Fable<sup>7</sup>

<sup>1</sup>*ITER Organization, Route de Vinon-sur-Verdon, 13067 St Paul Lez Durance, France*

<sup>2</sup>*Atominstitut, Technische Universität Wien, Stadionallee 2, 1020 Vienna, Austria*

<sup>3</sup>*CCFE, Culham Science Centre, Abingdon, OX14 3DB, United Kingdom*

<sup>4</sup>*General Atomics, P.O. Box 85608, San Diego, CA 92186-5608, USA*

<sup>5</sup>*CEA, IRFM, F-13108 Saint-Paul-lez-Durance, France*

<sup>6</sup>*PIIM-UMR 7345-Université d'Aix-Marseille-CNRS, 13397 Marseille Cedex 20, France*

<sup>7</sup>*Max-Planck-Institut für Plasmaphysik, Boltzmannstr. 2, D-85748 Garching, Germany*

### **1. Introduction**

ITER will start its operation in the non-active phase (H/He plasmas) with a W divertor allowing research on physics issues related to high Z impurity transport and control, which are essential for the achievement of the  $Q = 10$  mission, to be already undertaken in this phase. Lack of impurity control could lead to the radiative collapse of plasmas by W accumulation and increased disruptivity, which is detrimental to ITER operation. Control of W in H-mode plasmas requires, as a first step, the control of W production and its transport into the core plasma through the SOL and edge transport barrier. In addition, even when the concentration of W at the pedestal is kept at low levels, unfavourable core W transport can lead to its uncontrolled accumulation and to loss of the H-mode due increased radiation in present experiments (e.g. JET and ASDEX-Upgrade) [1-2], where schemes have been developed to avoid W accumulation by the application of additional heating to provide stable H-mode operation with W plasma facing components.

To evaluate if W accumulation is expected in ITER plasma scenarios and whether the available heating systems can provide the degree of control required for stable H-mode operation, a series of experiments have been performed in present tokamaks that address the ITER-specific aspects of W production and transport and their findings compared with modelling predictions whose results will be presented at this conference [3-7]. In this paper, we report on the results of the application of two of these integrated plasma models (ASTRA and JINTRAC, supplemented with dedicated studies with the NEO neoclassical transport code) to a wide range of H-mode plasma conditions in ITER, including confinement transients (i.e. H-L transitions). The simulations carried out deal with W transport in the core plasma of ITER in order to predict and to study how to avoid conditions in which core W accumulation can take place in ITER. Therefore, the pedestal W density is used to normalize the results obtained in our modelling with the modelled levels of W being kept low to identify when W accumulation takes place rather than to describe the post-accumulation plasma evolution. Prediction of the absolute level of the W density in ITER requires fully integrated simulations including the production of W at the divertor, its prompt redeposition, and its transport through the SOL and edge transport barrier, including the effects of ELMs, which have not yet been performed due to their complexity.

### **2. Modelling of core plasma W transport in stationary H-mode phases of ITER scenarios**

#### **2.1. Modelling of W transport for 7.5/2.65T and 15 MA/5.3T H-modes**

Simulations for ITER have been carried out with ASTRA and JINTRAC for stationary H-mode plasmas from 7.5 MA to 15 MA with transport being described with the GLF23 model for the anomalous part and NCLASS for the neoclassical part. Similar to the results of

simulations for present experiments [1, 4], plasma transport is found to be anomalous for most of the plasma cross section, except in the central region of the plasma where temperature and density gradients are lower. In particular, W transport in the central plasma region corresponds to neoclassical levels with very low values of diffusion coefficients and pinch velocities in ITER (typical values are  $D_W^{\text{neo}} \sim 5\text{-}10 \cdot 10^{-3} \text{ m}^2/\text{s}$  and  $v_W^{\text{neo}} \sim 1\text{-}5 \cdot 10^{-2} \text{ m/s}$ ). Outside this region W transport is anomalous with a very small inward anomalous pinch, as shown in Fig. 1. This leads to very weakly peaked W density profiles away from the central plasma region, much less peaked than the DT and electron density profiles for which the inward DT flux predicted by GLF23 is much larger for the collisionalities typical of ITER plasmas (see Fig. 1). The extent of the central region where anomalous transport is suppressed depends on the model used to describe anomalous transport. For the GLF23 model and the typical ITER plasma parameters, this is found to be dependent on fine details of the q profile and its shear in the central plasma region, which are difficult to predict for ITER. Two types of conditions are typically found: one in which the region with low W anomalous transport is very small ( $r/a \leq 0.05$ ) and another in which the region with low W anomalous transport is wider ( $r/a \leq 0.2\text{-}0.3$ ). For the former, the W density profiles develop no or a very small level of central peaking both for steady state and H-L transient phases, while, for the latter, a moderate degree of W central peaking is found for stationary H-modes and large W central peaking can be found for H-L transient phases. In this paper, we concentrate our analysis on the conditions for which anomalous transport is predicted to be suppressed in  $r/a \leq 0.2\text{-}0.3$ , for which central W peaking is expected to be largest, and evaluate the possibilities for its control with the heating and fuelling systems available at ITER. The studies carried out do not consider the effects of sawteeth, as these are predicted to be very infrequent in ITER due to their stabilization by fast particles, nor of other MHD modes whose effect on core W transport can be significant. These effects are generally favourable for W transport (i.e. they expel W from the core plasma) [4] and thus our studies can be considered conservative in this respect. Similarly, as mentioned in the introduction, expulsion of W by ELMs is not modelled and the pedestal plasma parameters are assumed to be stationary in time, which is a good approximation for a suppressed/controlled ELMy H-mode regime in ITER.

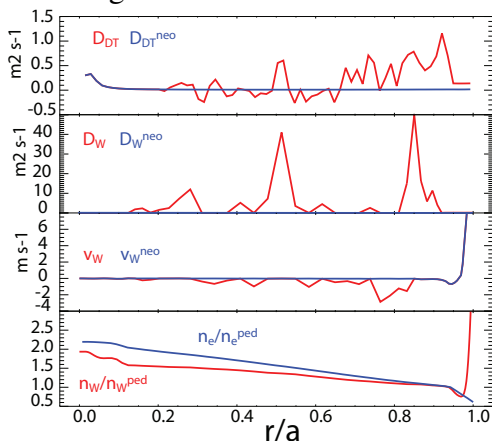


Fig. 1. JINTRAC-modelled transport coefficients for DT and W in an ITER  $Q = 10$  plasma and resulting normalized electron density and W density profiles. The contribution of neoclassical transport to the coefficients is shown.

Neoclassical transport studies for ITER H-mode plasmas with NCLASS and NEO have shown that a moderate inward pinch exists for both D and T in the central plasma region due to the different masses of D and T, as shown in Fig. 2. This leads to the appearance of a moderate density gradient and inward convective DT particle fluxes (compensated by

In the central plasma region, where W transport is dominated by neoclassical effects, the W density profile shape is influenced by the gradients of the DT density and temperature. In this respect, the ITER H-mode plasmas are qualitatively different from existing devices (except plasmas not heated by NBI) because the central particle source provided by ITER's 1 MeV NBI is very small compared to present devices (more than  $10^2$  times lower than for JET plasmas at the same levels of  $P_{\text{NBI}}$ ). This results in lower predicted core DT gradients for ITER and in these gradients being mostly determined by neoclassical transport physics rather than NBI particle sources.

outward diffusive fluxes) which are much larger than those resulting from the deposition of NBI particles in this region ( $3 \cdot 10^{17} \text{ m}^{-2}\text{s}^{-1}$  inward neoclassical DT particle flux at  $r/a = 0.2$  compared with an outflux from NBI deposition of  $\sim 5 \cdot 10^{16} \text{ m}^{-2}\text{s}^{-1}$  at the same location). The relation between the neoclassical transport self-consistently established DT density gradients and the corresponding DT temperature gradients determines the W density profile in the ITER central plasma through the inward driven density-gradient pinch and the outward-driven temperature screening.

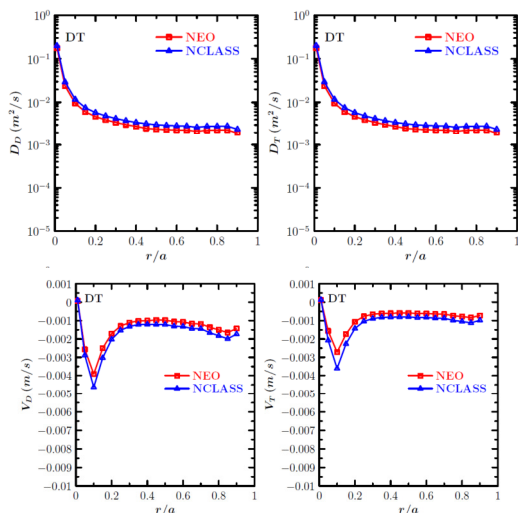


Fig. 2. Modelled neoclassical transport coefficients ( $D$  top,  $V$  bottom) for  $D$  (left) and  $T$  (right) for an ASTRA-modelled ITER  $Q = 10$  plasma showing an inward pinch for  $D$  and  $T$  in the central plasma region.

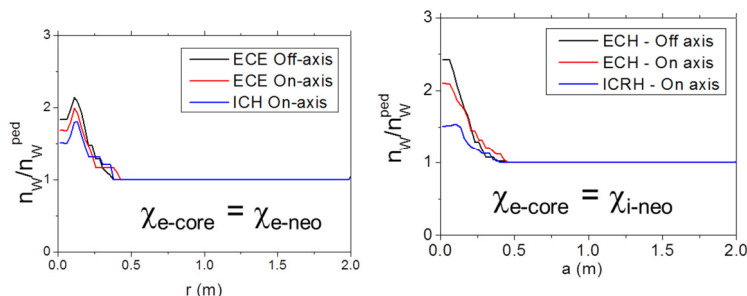


Figure 3.  $W$  density profiles, normalized to the pedestal, for ITER  $Q = 10$  plasmas with 33 MW of NBI and 20 MW of RF for a range of heating schemes modelled with ASTRA. Core particle and energy transport assumptions are those of neoclassical transport for DT ions and two assumptions are explored for electron transport.

profiles being somewhat more peaked for the configurations with lower central power density (Fig. 4). The lower  $\langle n_e \rangle$  in 7.5 MA H-modes than in 15 MA plasmas leads to weaker coupling of the electron and ion temperatures and to a larger  $T_e/T_i$  and, therefore, to a stronger sensitivity of the results to assumptions on the central level of electron thermal transport.

Due to the key role of neoclassical transport and not of NBI sources in the determination of the main ion density profiles in the ITER central plasma region, the physics of core  $W$  peaking is different in He or D H-mode plasmas than in DT plasmas. This is due to the fact that the magnitude of the predicted neoclassical inward pinch for single main ion plasmas is much smaller than for DT plasmas. As a consequence, the core D density profiles are found to be much flatter and the  $W$  density profiles to be hollow in the central region for D plasmas, unlike for DT (see Fig. 5 for an example of 7.5MA/2.65T D and DT plasmas).

ASTRA and JINTRAC modelling find that, for 15 MA  $Q \sim 10$  plasmas with  $P_{\text{NBI}} \sim 33$  MW and  $P_{\text{RF}} \sim 20$  MW (ECRH or ICRH), the level of core  $W$  peaking in ITER is very modest for a wide range of assumptions regarding electron thermal transport in the central plasma region (see Fig. 3), which is in agreement with ITER-like experimental results in Alcator C-Mod [3]. This modest level can be further reduced by ITER's H&CD systems even for  $Q \sim 10$  plasmas, because the ITER RF heating systems can provide very peaked power deposition profiles so that the electron (ECRH) and ion (ICRH-He<sup>3</sup> minority) power densities exceed those of alpha heating in the central plasma region, despite the power deposited by each of these two systems being only 20% of the total alpha heating, which, thus, can modify the

central temperature and density profiles. Modelling of 7.5 MA/2.65T DT plasmas shows similar results regarding  $W$  transport and  $W$  density profiles as those for 15 MA  $Q = 10$  plasmas. In this case, the differences between the various possibilities explored is larger ( $P_{\text{NBI}} = 33$  MW and  $P_{\text{RF}} = 0$  and 20 MW (ECRH or ICRH)) with the  $W$  density

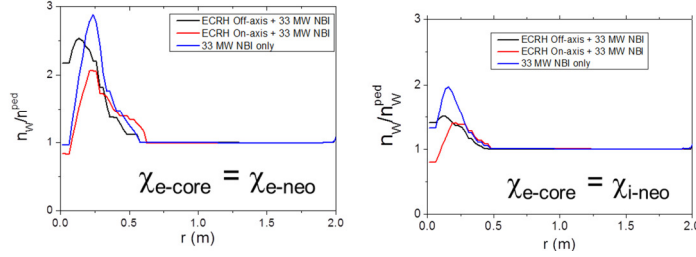


Figure 4.  $W$  density profiles, normalized to the pedestal value, for ITER 7.5MA/2.65T plasmas with 33 MW of NBI and 0/20 MW of RF for a range of heating schemes modelled with ASTRA. Core particle and energy transport assumptions are those of neoclassical transport for DT ions and two assumptions are explored for electron transport.

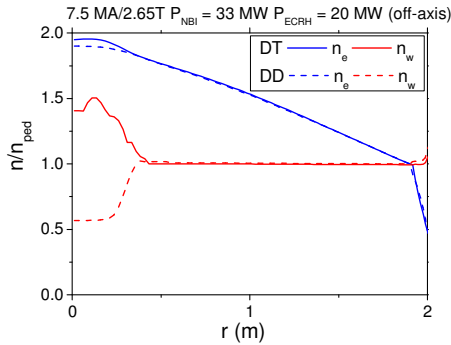


Figure 5. Electron and  $W$  density profiles, normalized to the pedestal, for ITER 7.5MA/2.65T plasmas with 33 MW of NBI and 20 MW of ECRH for DT and DD modelled with ASTRA.

impurity transport in present experiments [10]. One of them is the centrifugal force effect due to the toroidal rotation of impurities dragged by the main DT ion flow (which can become supersonic for high  $Z$  impurities) and the other is the effect of high energy particles, which are ubiquitous in ITER plasmas (3.5 MeV alpha particles, 1 MeV NBI ions and ICRH accelerated minority ions). These two effects have been modelled with the NEO code [11] using plasma parameters (including toroidal rotation profiles) and fast particle energies from ASTRA, as well as energy distributions from ICRH-accelerated ions calculated following the same approach as in [12]. NEO simulations show that both the diffusion and pinch velocity for  $W$  increase in the same proportion with the plasma toroidal rotation velocity so that the  $W$  core density peaking remains constant for a wide range of Mach numbers (up to  $M_{DT} = 0.4$ ); for larger Mach numbers, the pinch velocity decreases and can reverse sign, which would be beneficial for  $W$  control in ITER. It should be noted that the toroidal rotation Mach number predicted by ASTRA and JINTRAC is very low for ITER ( $M < 0.1$ ) due to the low momentum input provided by the 1 MeV NBI in ITER. Thus, no major effect of toroidal rotation on  $W$  transport is expected in ITER (i.e. the simulations carried out with NCLASS for ITER are appropriate) unless intrinsic toroidal rotation is very large in ITER, which does not appear likely. Therefore, rotation effects are expected to have little influence on the stationary  $W$  profiles that will be achieved in ITER H-modes (although they will affect the speed at which stationarity is reached), unless very large toroidal Mach numbers are achieved, in which case, they will reduce  $W$  peaking compared to the results above.

Similarly, analysis of the effects of fast particles on  $W$  transport shows that these are negligible for alpha particles and NBI ions in ITER due to their large energy, low density,

It has been recently pointed out that electron-scale turbulent processes may have an effect on energy and particle transport at larger spatial scales [8]. An initial evaluation of this effect for ITER  $Q \sim 10$  conditions has been performed with ASTRA and anomalous transport being modelled by the TGLF model, including the saturation of multi-scale

turbulence [9]. This leads to a much larger predicted level of  $W$  anomalous transport in the central plasma region compared to the GLF23 results above and to the resulting strongly hollow  $W$  density profiles in ITER. Further detailed studies for lower plasma currents and other plasma conditions are in progress.

## 2.2. Modelling of effects of toroidal rotation and fast particles on neoclassical $W$ transport

The calculations carried out with ASTRA and JINTRAC in the previous section contain a simplified model for neoclassical  $W$  transport (NCLASS) that does not describe effects that have been identified to be important for high  $Z$

and moderate density and energy radial gradients. On the contrary, the effects associated with T and He<sup>3</sup> ions accelerated by ICRH for 5.3 T (first-harmonic He<sup>3</sup> and second-harmonic T) are significant, both because of their moderate density ( $n_{\text{He}^3}/\langle n_e \rangle \sim 2\%$ ,  $n_{\text{T-fast}} \sim 5\%$ ) and the very steep radial temperature gradients, which result from the ICRH power being absorbed in a resonant layer, as shown in Fig. 6. The temperature screening provided by these steep radial temperature gradients can act positively on core W transport and can even reverse the sign of the inward pinch (i.e. leading to hollow W density profiles) for the highest levels of  $P_{\text{ICRH}}$  considered (20 MW) and He<sup>3</sup> concentrations modelled (2%). However, this positive effect is not constant across the central part of the plasma and depends on the detailed shape of the fast-ion radial temperature profiles, so that, depending on the RF power, the concentration of He<sup>3</sup>, and the radial location in the resonant layer, the effects on W transport of ICRH-produced fast particles can be positive (i.e. W de-peaking), neutral, or negative (further W peaking). From the results of the present study, only at power levels of 20 MW with He<sup>3</sup> concentrations above 2%, it can be ensured that the effects on W transport of ICRH-accelerated particles are favourable across the whole resonant layer ( $r/a \leq 0.15$ ), as shown in Fig. 7. Self-consistent simulations with NEO in ASTRA and/or JINTRAC and including the effects of fast ICRH-accelerated ions on W neoclassical transport are required to provide a more precise evaluation of the possible advantage of ICRH with respect to ECRH heating for W control.

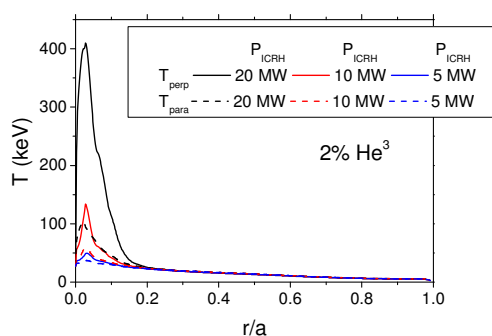


Fig. 6. Modelled perpendicular and parallel temperature radial profiles of the ICRH-accelerated fast He<sup>3</sup> ions for ITER  $Q = 10$  plasma conditions and a range of ICRH powers (2% He<sup>3</sup>).

### 3. Modelling of W transport in H-mode exit phases of ITER scenarios.

While the situation regarding core W peaking and control during the stationary phases of ITER H-modes evaluated in the previous section is rather positive, this is much more challenging for the termination phase of H-modes in ITER, which is in qualitative agreement with experimental evidence. To assess this issue and to explore the possibilities for the avoidance

of W accumulation during H-mode termination phases, JINTRAC simulations have been carried out. In these simulations, core transport is modelled with the same assumptions as in section 2 for the H-mode phase, while the Bohm/gyro-Bohm model is used to describe anomalous transport in the L-mode phase. The simulations include a model for transport in the H-mode transport barrier and its modification with the edge power flow margin above

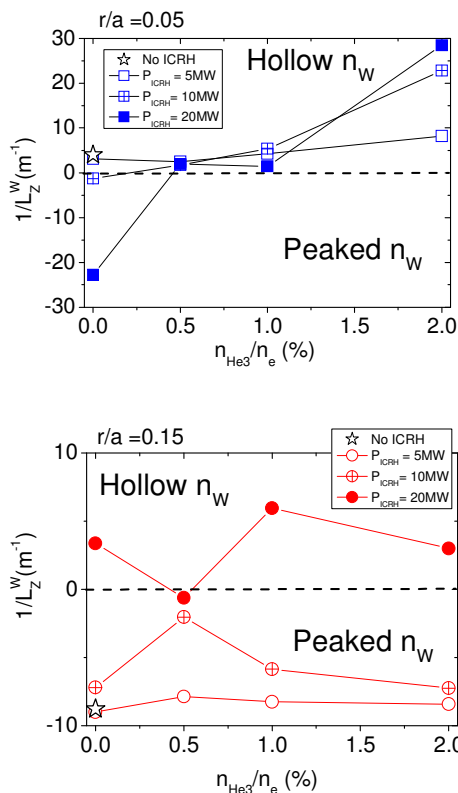


Fig. 7. NEO-modelled inverse scale-lengths of the W density profile at two positions in the resonant layer of ICRH for ITER  $Q = 10$  plasmas for  $P_{\text{ICRH}} = 5\text{-}20$  MW and  $n_{\text{He}^3}/n_e = 0 - 2\%$ .



the L-H power threshold, which has been found to describe well experimental behaviour [13]. The plasma pedestal parameters are assumed to be limited by the self-consistently calculated edge MHD stability limit (corresponding to controlled/suppressed ELMy H-mode conditions in ITER) and the separatrix plasma density and temperature are obtained from scalings derived from edge plasma codes following an approach similar to [14].

Termination of H-mode plasmas presents specific challenges due to the relatively slow timescale for the control of the radial position of ITER plasmas compared to that of the decrease of the plasma energy ( $W_{\text{plasma}}$ ), which can lead to contact between the plasma and the high field side first wall in these phases [15]. Optimum radial position control requires a slow decrease of the plasma energy in the H-mode termination phase, which can be achieved by extending the time that the plasma remains in H-mode during the termination phase. This requires sustaining an edge power flow as high as possible above the L-H transition threshold as long as possible [15], which can be achieved by switching-off pellet fuelling, thus reducing the plasma density, when the ramp-down of the additional heating starts and by maintaining some lower level of additional heating after that. This strategy also favours the sustainment of high  $P_{\alpha}$  in the H-mode termination phase as the core plasma temperature remains high [15]. Simulations of  $W$  transport for the exit phase of  $Q \sim 10$  H-modes show that, while this strategy is very effective in minimizing  $dW_{\text{plasma}}/dt$ , it can lead to  $W$  accumulation in the core due to the steep density gradients formed in the plasma core following the stop of pellet fuelling (see Fig. 8). On the other hand, reducing the pellet fuelling in a more gradual way is sufficient to avoid  $W$  accumulation, while still providing a slow decrease of  $W_{\text{plasma}}$  in this phase (Fig. 8).

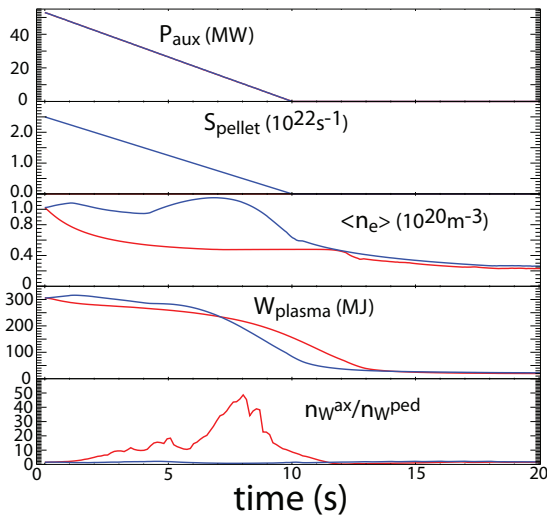


Figure 8. Evolution of auxiliary heating power, pellet fuelling and plasma parameters (energy, density and  $W$  peaking) in the termination phase of ITER  $Q=10$  plasmas for a 10s ramp of the auxiliary heating power and two fuelling pellet waveforms (immediate switch-off and 10s ramp-down).

keep density gradients low in the central plasma region during the H-mode termination phase. The most effective way to achieve this is to decrease the value of the plasma density itself to  $\langle n_e \rangle / n_{\text{GW}} \sim 0.5$  before the H-mode termination phase starts. This is found to effectively prevent  $W$  accumulation, even for a slow ramp-down of the heating power of  $\sim 20$ s for 7.5 MA and 15 MA plasmas, even when pellet fuelling is switched-off at the start of the power ramp-down, as shown in Fig.10. For the  $Q = 10$  scenario, this would correspond to a transition to a  $Q \sim 5$  phase by decreasing the pellet fuelling before the main auxiliary heating is ramped down, which would shorten the  $Q = 10$  burn length by 20-30 s.

The optimum way to ramp the power versus pellet fuelling in ITER to achieve a slow decrease of  $W_{\text{plasma}}$  and to avoid  $W$  accumulation depends on the plasma scenario, as the magnitude of the core neoclassical peaking depends on the plasma parameters themselves. For instance, for 7.5 MA/2.65T DT H-mode plasmas with  $\langle n_e \rangle / n_{\text{GW}} \sim 0.85$ , for which  $P_{\alpha}$  is low, it is found that switching off pellet fuelling and ramping down the power slowly is already sufficient to avoid large  $W$  accumulation (Fig. 9). Ramping down the pellet fuelling together with the heating in this case reduces  $W$  peaking in the initial phase of the H-mode termination but increases it towards the later phase near the H-L transition (Fig. 9).

It is important to note that, as mentioned earlier, the key to avoid  $W$  accumulation is to

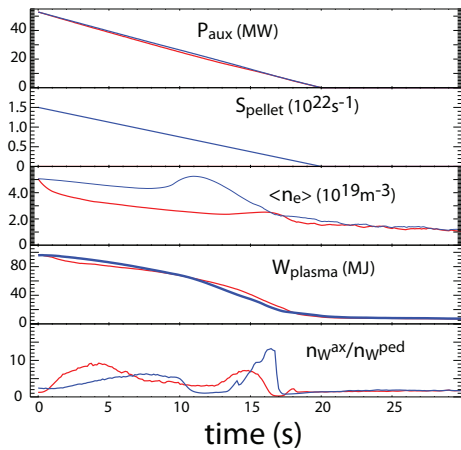


Figure 9. Evolution of auxiliary heating power, pellet fuelling and plasma parameters (energy, density and W peaking) in the termination phase of ITER 7.5 MA/2.65T plasmas for a 20s ramp of auxiliary power and two fuelling pellet waveforms (immediate switch-off and 20s).

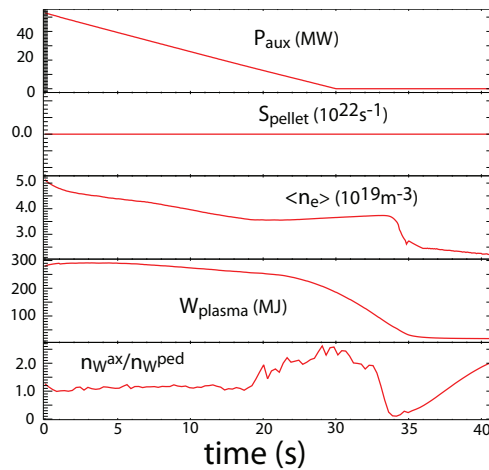


Figure 10. Evolution of auxiliary heating power, pellet fuelling and plasma parameters (energy, density and W peaking) in the termination phase of ITER  $Q \sim 5$  ( $\langle n_e \rangle = 0.5 n_{GW}$ ) plasmas for a 30s ramp of auxiliary heating power and immediate pellet fuelling switch-off.

As mentioned in section 2, very low quantities of W have been assumed in these studies to maintain a low level of W radiation, which allows the modelling of the accumulation of W in the H-mode termination phase and its expulsion in the L-mode phase. For higher W levels, the radiation by W affects the edge power flow, which, in turn, reduces the edge power flow and the duration of the H-mode termination phase. To model the dynamics of ITER plasma in which W accumulation takes place in this phase, a series of studies have been carried out with higher W densities. Stationary  $Q = 10$  plasmas with W concentrations at the pedestal top of up to  $4 \cdot 10^{-5}$  have been produced by assuming given levels of W influx. Following the achievement of stationary conditions, the auxiliary heating power is ramped down and pellet fuelling is switched off, which leads to W accumulation in the H-mode termination phase, and the W density evolution and W radiation has been modelled. These simulations show that, despite large values of the W density and central W radiation due to accumulation, the total radiated power remains moderate due to the large values of electron temperature that the plasma reaches in ITER during the H-mode termination (due to the decrease of plasma density), as shown in Fig. 11. In particular, it has not been possible to obtain ITER simulations with “classical” inverted  $T_e$  profiles that are associated with the termination of plasmas by W accumulation in present experiments, as shown in Fig. 12. When large edge W influxes are applied in the modelling of the H-mode termination phase, a thermal collapse of the edge plasma and not of the central plasma is obtained in the simulations. This indicates that the termination of H-mode plasmas by W accumulation in ITER may be qualitatively different from present experiments due to the lower radiation efficiency of W in the ITER central plasma region, which reaches electron temperatures well above 10 keV in these phases, and the good temperature screening of W in the pedestal region, which leads to very large W concentrations there.

#### 4. Conclusions

Integrated plasma modelling including W transport for stationary ITER H-modes and for H-mode terminations has been carried out for a range of plasma conditions from 7.5MA/2.65T to 15MA/5.3T. The simulations show that very low levels of core W density peaking are expected in ITER during stationary H-modes due to the low central density gradients and the associated very low particle source from ITER’s 1 MeV NBI. The density gradients in the central plasma region are determined by neoclassical transport and are largest for DT plasmas than for D plasmas, thus easing W control in the operational phase before DT. On

the contrary,  $W$  accumulation is found to readily occur in the termination phase of ITER H-modes if no optimization of the additional heating ramp-down versus pellet fuelling switch-off is considered.  $W$  accumulation can be avoided by adjusting the rates of power versus pellet fuelling in the ramp-down, with the adjustment dependent on plasma conditions. An alternative way to terminate the H-modes, which is found to be very robust to  $W$  accumulation, is to introduce a low density H-mode phase with  $\langle n_e \rangle / n_{GW} \sim 0.5$  after the main high density phase of ITER plasma scenarios and then ramp-down the additional heating. Simulations of plasma termination by  $W$  accumulation in ITER have been performed. Initial results of these simulations show that, due to the high temperatures of ITER plasmas, core  $W$  radiation remains limited even when relatively strong  $W$  accumulation takes place. Due to this effect, the formation of hollow temperature profiles, a signature of  $W$  accumulation in present experiments with lower plasma temperatures, cannot be achieved in our ITER modelling. This indicates that the termination of discharges suffering from  $W$  accumulation in ITER may be different than in present devices where disruptions are found to occur. Obviously, the quantitative accuracy of our predictions for ITER depends on the validity of the models used. In this respect, comparisons of predictions of our modelling tools with present experiments, such as reported in [4-7] are key to our understanding of  $W$  transport in ITER plasmas. Of particular importance is to quantitatively determine the role of NBI particle sources, neoclassical, and anomalous core transport in determining  $W$  density profiles in present experiments and ITER. If the predicted levels of anomalous transport in the ITER core by models such as [9] can be confirmed, this would result in  $W$  accumulation not taking place in ITER and DEMO, provided that the pedestal  $W$  density can be controlled through ELM control schemes.

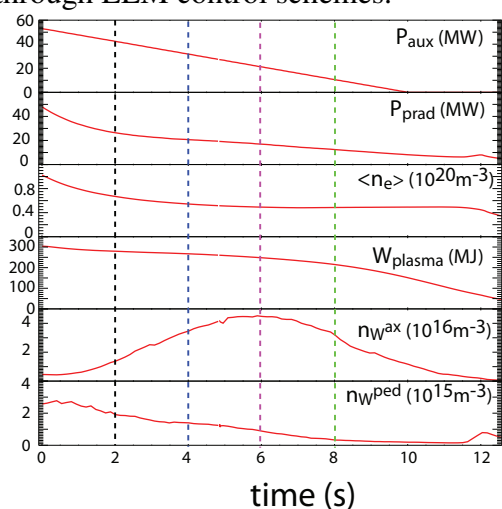


Figure 11. Evolution of auxiliary heating power, radiated power and plasma parameters (electron density, energy, axial and pedestal  $W$  densities) in the termination phase of ITER  $Q=10$  plasmas for a 10s ramp of the auxiliary heating power with immediate pellet fuelling switch-off.

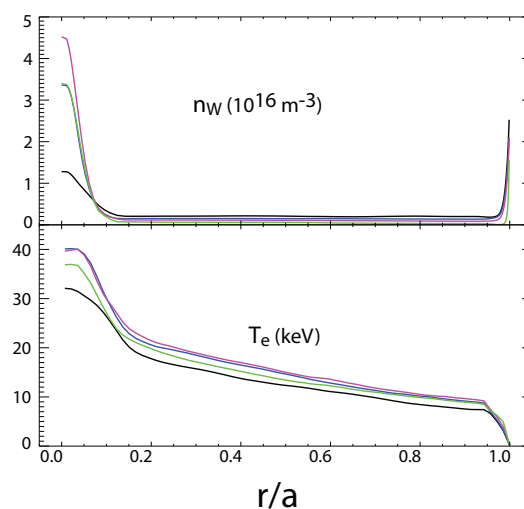


Figure 12.  $W$  density and electron temperature profiles at various times (those marked in Fig. 11) in the termination phase of ITER  $Q=10$  plasmas for a 10s ramp of the auxiliary heating power with immediate pellet fuelling switch-off.

Disclaimer: ITER is the Nuclear Facility INB no. 174. The views and opinions expressed herein do not necessarily reflect those of the ITER Organization

## 5. References

- [1] C Angioni, et al, Nucl. Fusion **54**(2014)083028.
- [2] R Dux, et al, PPCF **45**(2003)1815.
- [3] A Loarte, et al, Phys. Plas. **22**(2015)056117.
- [4] C. Angioni, et al., this conference.
- [5] M. Valisa, et al., this conference.
- [6] F. Köchl, et al., this conference.
- [7] M. Reinke, et al., this conference.
- [8] N T Howard, et al, Phys. Plas. **21**(2014)112510.
- [9] G. Staebler, TTF 2016
- [10] FJ Casson, et al, PPCF **57**(2015)014031.
- [11] E Belli, et al, PPCF **54**(2012)015015.
- [12] RJ Dumont, et al, Nucl. Fusion **53**(2013)013002
- [13] F. Köchl, et al., submitted to Nucl. Fusion
- [14] A. Polevoi, et al., Nucl. Fusion **55**(2015) 063019.
- [15] A. Loarte, et al., Nucl. Fusion **54**(2014) 123014.